

# INTERNATIONAL SOCIETY FOR SOIL MECHANICS AND GEOTECHNICAL ENGINEERING



*This paper was downloaded from the Online Library of the International Society for Soil Mechanics and Geotechnical Engineering (ISSMGE). The library is available here:*

<https://www.issmge.org/publications/online-library>

*This is an open-access database that archives thousands of papers published under the Auspices of the ISSMGE and maintained by the Innovation and Development Committee of ISSMGE.*

*The paper was published in the proceedings of the 20<sup>th</sup> International Conference on Soil Mechanics and Geotechnical Engineering and was edited by Mizanur Rahman and Mark Jaksa. The conference was held from May 1<sup>st</sup> to May 5<sup>th</sup> 2022 in Sydney, Australia.*

## Performance degradation of high-speed railway foundation due to train traffic loading and rainfall infiltration

Dégradation des performances des fondations du chemin de fer à grande vitesse en raison de la charge du trafic ferroviaire et de l'infiltration des précipitations.

**Xuecheng Bian, Ying Wu, Jianqun Jiang & Yunmin Chen**

*Key Laboratory of Soft Soils and Geoenvironmental Engineering, MOE, Department of Civil Engineering, Zhejiang University, Hangzhou, China, bianxc@zju.edu.cn*

**ABSTRACT:** Extreme weathers, such like heavy rainfall, are becoming more frequent in southeast China where high-speed rail lines densely deployed in recent decades, and bringing huge challenges to the durability of these transportation infrastructures. Water infiltration into railway foundation due to heavy rainfall is one of major factors leading to performance degradation in high-speed railways in addition to repeated train traffic loadings. This paper presents a full-scale physical model test on a high-speed railway with different water contents in soils in the track foundation. The tests were conducted in the high-speed railway testing apparatus developed in Zhejiang University. The size of the testing box in the experiment is 15m long, 6m wide and 5m high. A portion of full-scale high-speed railway was constructed in the test box. The highest train speed in the model test was up to 360km/h. Both pore water pressure buildup in the track foundation and excessive track settlement development are reproduced. Test results show that rainfall infiltration into railway formation can cause significant performance degradation of the railway, indicated by the loss of foundation stiffness and excessive accumulative settlement. Accumulative settlement in railway foundation grows remarkably accompanied by the development of pore water pressure in the model tests. The test results indicate that reducing rainfall infiltration in railway foundation or improving water drainage in the track foundation is critical for keeping high-speed railways in stable state.

**RÉSUMÉ :** Les conditions météorologiques extrêmes, telles que les fortes pluies, sont de plus en plus fréquentes dans le sud-est de la Chine, où les lignes ferroviaires à grande vitesse se sont densément déployées au cours des dernières décennies, et posent d'énormes défis à la durabilité de ces infrastructures de transport. L'infiltration d'eau dans les fondations du chemin de fer en raison de fortes pluies est l'un des principaux facteurs menant à la dégradation des performances des chemins de fer à grande vitesse, en plus des charges répétées du trafic ferroviaire. Cet article présente un essai de modèle physique à grande échelle sur une voie ferrée à grande vitesse avec différents teneurs en eau dans les sols de la fondation de la voie. Les tests ont été menés dans l'appareil d'essai ferroviaire à grande vitesse mis au point à l'Université du Zhejiang. La taille de la boîte de test dans l'expérience est de 15 m de long, 6 m de large et 5 m de haut. Une partie du chemin de fer à grande vitesse à grande échelle a été construite dans la boîte d'essai. La vitesse de train la plus élevée lors du test sur modèle était de 360 km / h. L'accumulation de pression d'eau interstitielle dans la fondation de la voie et le développement excessif de tassement de voie sont reproduits. Les résultats des tests montrent que l'infiltration des précipitations dans la formation ferroviaire peut entraîner une dégradation significative des performances de la voie ferrée, indiquée par la perte de rigidité des fondations et un tassement accumulé excessif. Le tassement accumulé dans les fondations ferroviaires croît remarquablement accompagné du développement de la pression interstitielle de l'eau dans les essais sur modèle. Les résultats des tests indiquent qu'il est essentiel de réduire l'infiltration des précipitations dans les fondations des chemins de fer ou d'améliorer le drainage de l'eau dans les fondations des voies pour maintenir les chemins de fer à grande vitesse dans un état stable.

**KEYWORDS:** Full-scale test, water level, train speed, accumulative settlement

### 1 INTRODUCTION.

In recent years, extreme weather has become more frequent, especially intense precipitation, which has brought serious losses to transportation infrastructures around the world. Railway foundation are not only subject to the long-term train cyclic loading, but also exposed to high water table from heavy rainfall. Subgrade failures, such as mud pumping, progressive shear failure and excessive plastic deformation, are more likely to occur due to the combined effect of the pore water and train loads (Li and Selig, 1998). Performance degradation in high-speed railway would cause serious railway accidents and affect people's travel (Gitirana Jr, 2005).

The influence of water infiltration on subgrade performance cannot be ignored. Much research has been carried out through triaxial tests to investigate the influence of water content on subgrade soil. The resilient modulus which is significantly affected by water content is an important parameter to evaluate the stiffness of subgrade soil since it can reflect the ability of subgrade to resist deformation. Test results have shown that moisture content plays a role in lubricating the soil particles in the subgrade. Matrix suction can mitigate the lubricating effect of soil particles to limit the sliding and rotation of particles when

in low water content so that the stiffness of subgrade is improved (Chen et al., 2020). The increase of the water content will reduce the soil cohesion, thus decreasing the resilient modulus of subgrade (Thom and Brown, 1987, Liu et al., 2019). Blackmore et al. (2020) found that when the saturation increases from 45% to 85%,  $M_R$  decreases from 467 MPa to 36.4 MPa. Beyond the optimum water content, the decrease in resilient modulus becomes more significant. Drumm et al. (1997) took 11 types of soils to prepare three samples with different moisture content for testing. They stated that the resilient modulus of soils decreases with the increase of water content, but the extent of decrease was related to the type of soil. Hicks and Monismith (1971) pointed that the resilient modulus of granular materials reduces as saturation increases under a given stress condition. Soil density, aggregate type and fine content also affect resilient modulus in some degree.

Pore water pressure and accumulative settlement would further develop due to the coupled effect of water infiltration and traffic loads. When the pore water pressure is high enough, the effective stress in the soil decreases, which may soften soil and cause soil deformation easily. Haynes (1961) stated that increasing the saturation from 60% to 80% doubled the axial permanent strain. Liu and Xiao (2010) pointed out that axial cumulative strain shows a marked increase with increasing water

content, and soil failure may happen in a certain water content at a high dynamic stress level. Huang et al. (2010) conducted a series of triaxial undrained tests on sample of saturated silty clay along the Beijing-Tianjin high-speed railway. They concluded that the generated excess pore pressure and residual shear strain of the specimens after long-term traffic load both can be regarded as the characterizations of damage degree of soil structure, and they all have their threshold values. Good drainage condition will enhance the bearing capacity of normally consolidated foundation. Miller et al. (2000) found that accumulated plastic deformation increased with the moisture content because of the development of pore water pressure. The result of field observations also showed that the deviator stress from train loading on the subgrade is easy to excess of the saturated shear strength after heavy rain, leading to progressive failure and excessive settlement, which results in the rapid track degradation.

The basic characteristics and stress-strain relationship of subgrade soil under certain stress conditions can be obtained through laboratory triaxial test. It contributes to understanding the influence of water content on subgrade soil and building up the basis of theoretical analysis. However, the overall stress state of the subgrade is variable, and the component of subgrade soil are interacted with each other. It is not enough to understand the overall macrodynamic characteristics of the subgrade just from the perspective of the soil element. Therefore, in order to investigate the combined effect of train load and water infiltration on the performance of subgrade, a full-scale physical model for ballastless railway was established. The water level in the subgrade were lifted or lowered by a water storage tank to simulate the variable of water content. Several typical water levels were studied to evaluate the performance of railway infrastructure.

## 2 TEST MATERIALS AND SETUP

### 2.1 Materials

The full-scale physical model of a ballastless railway was developed according to the high-speed railway design code used in China, including the dimension of the track structure and substructure, selection of materials, and requirement of compaction quality. Therefore, the experimental results from the model tests can be applied to evaluate the actual performance of high-speed railways. Fig. 1 shows the established full-scale physical model, consisting of the slab track structure and a 0.4 m thick roadbed, a 2.3 m thick subgrade and a 2.5 m deep subsoil. The axle load of simulated train was reach to 25t, and the speed was up to 360km/h. More detailed information can be referred to Bian et al. (2014a)

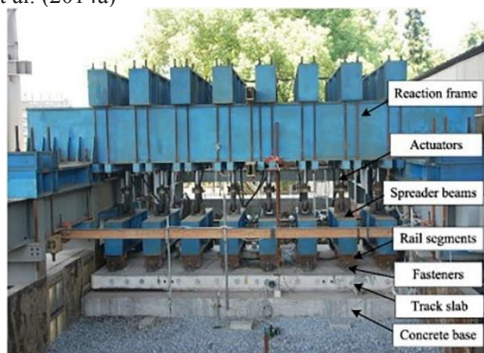


Figure 1. Full-scale physical model testing of slab track at Zhejiang University

The slab track structure was composed of rails, fasteners, track slab, CAM (cement asphalt mortar) layer and concrete base. CNH 60 rails were fixed to the track slab via eight pairs of WJ-7 type fasteners with a static stiffness of  $2.85 \times 10^7$  N/m. The

bending stiffness of rails was  $6.1 \times 10^6$  N·m<sup>2</sup>, and the distributed mass was 60 kg/m. Type of CRTS I slab was used in the experiment with sizes of 5.0 m×2.4 m×0.19 m. The bending stiffness of the track slab was  $4.0 \times 10^7$  N·m<sup>2</sup>, and the distributed mass was 950 kg/m. The concrete base, 5 m long, 3 m wide, and 0.3 m thick, was constructed in the test box with C40 concrete. The bending stiffness of the concrete base was  $1.9 \times 10^8$  N·m<sup>2</sup>, and the distributed mass was 1800 kg/m. CAM was poured into an infusion bag preplaced between the track slab and concrete base with the elastic modulus of  $1.0 \times 10^5$  kPa.

The substructure consisted of roadbed, subgrade and subsoil, which were filled with gravel, medium sand, and silty soil, respectively. The grain-size distributions of these three geomaterials are shown in Fig. 2. The maximum dry densities of the roadbed, subgrade and subsoil were 2.21 g/cm<sup>3</sup>, 2.11 g/cm<sup>3</sup> and 1.62 g/cm<sup>3</sup>, which corresponded to the optimum moisture contents of 4.2%, 4.0% and 18%, respectively. The subgrade and the subsoil were compacted at their optimum moisture contents. After the compaction of the roadbed and subgrade, soil was sampled at five locations at their surface. The relative compaction K (defined as the ratio of the dry density of the compacted soil to its maximum dry density), soil reaction K30 value and the second deformation modulus Ev2 were determined based on the static plate load tests using a circular plate with a diameter of 30 cm to verify the compaction quality.

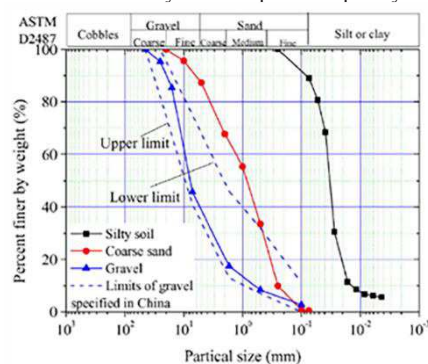


Figure 2. Grain-size distributions of geomaterials

### 2.2 Setup

Bian et al. (2014 b) presented a detailed description of the loading system for simulating train moving loads. The loading system was composed of a reaction frame, eight servo hydraulic actuators and eight spreader beams, as shown in Fig.1. Water levels in the physical model were raised and lowered using a movable water storage tank connected to a network of branch tubes at the bottom of the subsoil with a main supply tube as shown in Fig. 3. The performance of the railway infrastructure was evaluated at four typical water levels, i.e., (1) water level at the subsoil bottom, (2) water level at the subsoil surface, (3) water level at the subgrade surface and (4) water level falling back to the subsoil surface. The first case represents the normal design situation and the third case can simulate the submerged subgrade under extreme rainfall condition. Details of the configuration and measurement of the instrumentation in the railway substructure during the water level changes were described by Jiang et al. (2015)

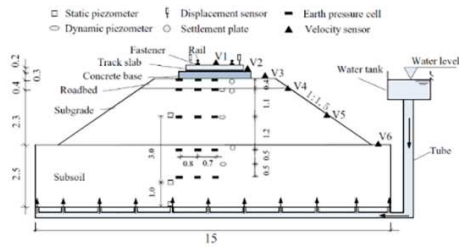


Figure 3. Cross-section of the physical model and configurations of instrumentations (unit: m).

### 3 RESULTS AND DISCUSSIONS

#### 3.1 Vibration velocity

Fig. 4 presents an increasing trend for the vibration velocity magnitude as train speeds increase from 5 km/h to 360 km/h. The vibration velocities of track structure and the roadbed were approximately linear increasing with the rates equal to 0.3 mm/s and 0.2 mm/s per 10 km/h. After water level rising, it was observed that the velocity magnitudes obviously higher than normal design situation. When the train speed exceeds 270km/h, the growth rate of vibration velocity at the track structure and roadbed increases significantly. At such high vibration velocity, the railway performance will get even worse under long-term traffic loadings, because larger deformations may develop.

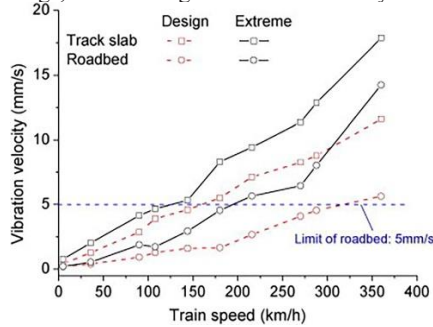


Figure 4. Vibration velocity magnitude versus train speed

#### 3.2 Contact pressure under track structure

Fig. 5 shows that the contact pressure distribution under track structure in design and extreme condition. The contact pressure was greatest at the edge of the track structure and decreased toward the center in design condition. This is consistent with the theoretical distribution of contact pressure below a rigid footing. Because the soil softens and support stiffness decreases when the subgrade saturated, the contact pressure below the track structure redistributed and became the shape of letter “W”. The train-induced contact pressure at the edge of concrete base was nearly zero, indicating that the soil around the edge entered into plastic state and cannot continue to bear the train load, so that the load on the edge is transferred to the rail and track center. The stress redistribution under track structure shows that the increase of water content will cause the expansion of the plastic zone of the soil, leading to the dynamic stability of roadbed decreased.

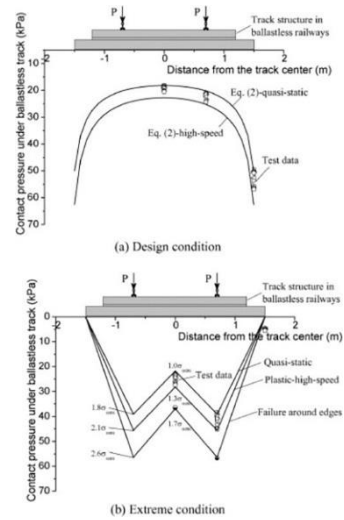


Figure 5. Contact pressure distribution below the track structure at the design and extreme conditions (a) Design condition (b) Extreme condition.

#### 3.3 Accumulated settlement

Fig. 6 represents the accumulative settlement in terms of number of passing axles measured at the surface of the track structure before and after water level rising. The cumulative settlement of the subgrade increases with the number of train passing axles and the growth of train speed. A rapid increase of the accumulative settlement occurred when the train moving loads at speed of 360 km/h. After water level rising, the accumulated deformation develops at a higher rate at both low speed and high speed, and showed no sign of slowing down. After 700,000 cyclic loadings at train speed of 360 km/h, the total accumulative settlement reached 76 mm, which was nearly 30 times as large as that before water level rising.

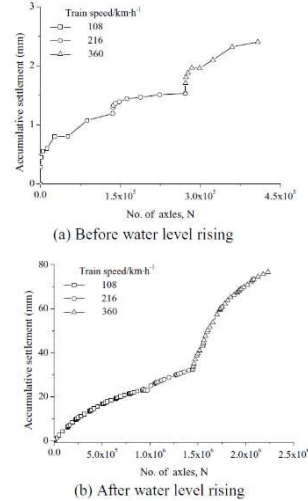


Figure 6. Accumulative settlement versus number of train passing axles

#### 3.4 Pore water pressure

Fig. 7 shows the dynamic pore water pressure measured in the subgrade and the subsoil. For the design condition, pore water pressure isn't exit. For the extreme rainfall condition, the pore water pressure can be dissipated in time because of the high permeability of the coarse sand in the subgrade. While the residual excess pore water pressure accumulates fast in subsoil and the train loads are supported by the soil skeleton and pore water pressure. When the train speed exceeds 300 km/h, the excess pore water pressure develops rapidly in the subsoil. As the train speed reaches 360 km/h, the dynamic pore water pressure

increased sharply to 2.5 kPa because the pore water inside soil has insufficient time to drain out under the impact loading from train's passages at high speeds.

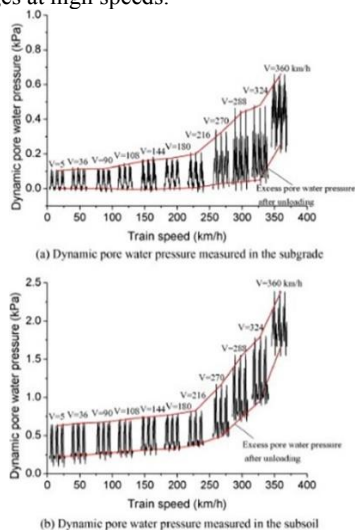


Figure 7. Development of the dynamic pore water pressure with increasing train speeds (a) Dynamic pore water pressure measured in the subgrade (b) Dynamic pore water pressure measured in the subsoil

#### 4 CONCLUSIONS

This paper presented an experimental study on a full-scale physical model to investigate the influence of water infiltration on the performance of ballastless high-speed railways. The following conclusions can be drawn based on the test results:

(1) The vibration velocity of track structure and roadbed increased significantly after the water level rising at the subgrade surface. The growth rates of the vibration velocity were almost identical for these two cases when the train speeds below 150 km/h. However, increasing train speeds led to faster growth rates of vibration velocities for the submerged subgrade, especially beyond 270 km/h.

(2) The contact pressure distribution under track structure changes from saddle shape to “W” shape in the submerged subgrade. The edge of concrete base is the first to enter plastic state and no longer to bear the load. The train load is transferred from the edge to the track center.

(3) The growth rate of accumulated settlement increased significantly in the subgrade after the water level rising and it's hard to reach a convergent stage. Especially under higher train speed of 360 km/h, the accumulative settlement of subgrade developed rapidly.

(4) The pore water pressure had no enough time to dissipate for low-permeability soil in the saturated subgrade, so that the train load is supported by pore water pressure and soil skeleton. The growth rates of pore water pressure increased with the train speed.

The railway embankment is always designed and constructed at the optimum moisture contents of the soil materials. In such ideal situation, the subgrade has a good drainage and the water content of subgrade soil is within a stable range. In fact, the railway is directly exposed to the atmosphere in the long-term service life. The increase in the water content will reduce the performance of the railway substructure, such as decreasing the strength and stiffness and increasing the dynamic soil stresses and vibrations. Such disadvantage situation should be considered during the railway design. Also, more theoretical investigations are required to reveal the degradation mechanism in railway formation with water's effect in the future.

#### 5 ACKNOWLEDGEMENTS

The financial support from the National Natural Science Foundation of China is gratefully acknowledged.

#### 6 REFERENCES

Bian X., Jiang H., Chen Y., et al. 2014a. A full-scale physical model test apparatus for investigating the dynamic performance of the slab track system of a high-speed railway. *Proceedings of the Institution of Mechanical Engineers, Part F: Journal of Rail and Rapid Transit* [J], 230: 554-571.

Bian X., Jiang H., Cheng C., et al. 2014b. Full-scale model testing on a ballastless high-speed railway under simulated train moving loads. *Soil Dynamics and Earthquake Engineering* [J], 66: 368-384.

Blackmore L., Clayton C.R.I., Powrie W., et al. 2020. Saturation and its effect on the resilient modulus of a pavement formation material. *Géotechnique* [J], 70: 292-302.

Chen W.-B., Feng W.-Q., Yin J.-H. 2020. Effects of water content on resilient modulus of a granular material with high fines content. *Construction and Building Materials* [J], 236.

Drumm E.C., Reeves J.S., Madgett M.R., et al. 1997. Subgrade resilient modulus correction for saturation effects. *JOURNAL OF GEOTECHNICAL AND GEOENVIRONMENTAL ENGINEERING* [J], 123: 663-670.

Gitirana Jr G. 2005. Weather-related geo-hazard assessment model for railway embankment stability [M].

Haynes J.H. 1961. Effects of repeated loading on gravel and crushed stone base course materials used in the AASHO Road Test.

Hicks R., Monismith C. 1971. Factors influencing the resilient response of granular materials. *Highway Research Record* [J].

Huang B., Ding H., Chen Y., et al. 2010. Experimental study of undrained strength property of saturated silty clay after traffic load [J]. *Chinese Journal of Rock Mechanics and Engineering*, 2010, 29(2): 3986 - 3993.

Jiang H., Bian X., Chen Y., et al. 2015. Impact of Water Level Rise on the Behaviors of Railway Track Structure and Substructure. *Transportation Research Record: Journal of the Transportation Research Board* [J], 2476: 15-22.

Li D., Selig E.T. 1998. Method for Railroad Track Foundation Design. I: Development. *Journal of Geotechnical & Geoenvironmental Engineering* [J], 124: 316-322.

Liu J., Xiao J. 2010. Experimental study on the stability of railroad silt subgrade with increasing train speed. *JOURNAL OF GEOTECHNICAL AND GEOENVIRONMENTAL ENGINEERING* [J], 136: 833-841.

Liu X., Zhang X., Wang H., et al. 2019. Laboratory testing and analysis of dynamic and static resilient modulus of subgrade soil under various influencing factors. *Construction and Building Materials* [J], 195: 178-186.

Miller G.A., Teh S.Y., Li D., et al. 2000. Cyclic Shear Strength of Soft Railroad Subgrade. *Journal of Geotechnical & Geoenvironmental Engineering* [J], 126: 139-147.

Terzaghi K. 1936. The shearing resistance of saturated soils. *Proc. 1st Int. Conf. Soil Mech.*, Cambridge, Mass., 1, 54-56.

Thom N., Brown S.F. 1987. Effect of moisture on the structural performance of a crushed-limestone road base [C].